RSC Advances

ROYAL SOCIETY OF CHEMISTRY

www.rsc.org/advances

Improvement of performance of Au-Cu/AC catalyst using thiol for acetylene hydrochlorination reaction

Guotai Hong[a], Xiaohui Tian[a], BinBo Jiang[*a], Zuwei Liao[a], Jingdai Wang[a], Yongrong Yang[ab], Jie Zheng[c]

[a.]State Key Laboratory of Chemical Engineering, College of Chemical and Biological Engineering, Zhejiang University, Hangzhou 310027, Zhejiang, China

[b.]Shanghai Key Laboratory of Catalysis Technology for Polyolefins, Shanghai 200062, China

[c.]Department of Chemical and Biomolecular Engineering, The University of Akron, Akron, Ohio, USA 44325

ABSTRACT

In order to overcome problems of Au-Cu bimetallic catalysts for acetylene hydrochlorination reaction such as instability, Au-Cu-SH/AC catalysts were prepared through the introduction of thiol and tested to examine their activity and stability. It was found that performances of Au-Cu-SH/AC catalysts were quite excellent, with significantly higher catalytic activity and better stability than performances of Au/AC and Au-Cu/AC catalysts. The content of Cu and thiol additives were also optimized and the optimum molar ratio of Au/Cu/SH was 1:1:10. Catalyst samples were characterized by scanning electron microscopy (SEM), nitrogen adsorption/desorption (BET), X-ray diffraction (XRD), transmission electronic microscopy (TEM), H_2 temperature-programmed reduction (H_2-TPR), and X-ray photoelectron spectroscopy (XPS). It was demonstrated that Au-Cu-SH/AC catalysts were Au^0-based catalysts, due to thiol can reduce Au^{3+} to Au^0 species during the preparation process. Au^0 species exhibited more

excellent catalytic activity than Au^{3+} species for acetylene hydrochlorination, according to the comparison with the composition of active species in different samples through XPS. Furthermore, the sulfydryl of thiol could bond to the surface of gold nanoparticles (Au NPs). It helped mitigating the oxidation of Au^0 by HCl, protecting Au NPs from structure damage, stabilizing Au NPs in a nearly constant particle size and keeping more active structure under the reaction ambience. Thus, better active species dispersity and active structure protection of Au NPs resulted in better catalytic activity and stability of Au-Cu-SH/AC.

Key word: Au-Cu catalyst; Thiol; Dispersity of Au NPs; Acetylene hydrochlorination;

---

* Corresponding author. E-mail addresses: Jiangbb@zju.edu.cn (Binbo Jiang).

1 Introduction

Along with the fast economic growth, the demand and consumption of polyvinyl chloride (PVC) in China grow quickly in recent years, and production of PVC reached 16.30 million tons in 2014[1]. Ethylene oxychlorination, a clean petroleum-based route to synthesize vinyl chloride monomer (VCM), is broadly used in developed countries. However, based on the energy structure and the rekindled enthusiasm in coal-derived feedstock, the coal-based process, acetylene hydrochlorination, is dominating the PVC industry of China. Statistically, acetylene hydrochlorination contributes to more than 70% of PVC production in China every year[2]. Acetylene hydrochlorination is catalyzed by hazardous Hg catalysts and 60% of Hg in China is consumed in this usage

annually. The volatilization of poisonous Hg during the reaction is severely harmful to the safety of the employees and environment[3][4]. Consequently, novel heterogeneous non-mercury catalysts have been widely investigated in the past decades[5][6][7][8][9], aiming at the substitution of their Hg counterparts. As a pioneer, Shinoda[4] had tested the catalytic activities of more than 20 kinds of metal chlorides in acetylene hydrochlorination reaction. By analyzing Shinoda's experimental results, Hutchings[6] drew the conclusion that the activity of different metal chlorides in acetylene hydrochlorination was correlated with the standard electrode potential of corresponding metal cations. Accordingly, he predicted that Au^{3+} might be the most active catalyst in this reaction in 1985, which was experimentally confirmed in 1988[10].

In recent years, Au catalysts have aroused huge concerns due to its excellent catalytic performance in various catalytic systems[11][12][13][14][15][16]. Along with these developments, the study of Au/AC catalyst for acetylene hydrochlorination has also made significant progress[8][17][18][19][20][21]. Most importantly, it is widely noticed that the poor stability and high cost of Au catalysts restrict its industrial application. For purpose of overcoming these two problems, researchers have made great efforts to adopt varied approaches, including carrier modification[7], design of the preparation method[19], and the introduction of additional metal components[9][20][21][22][23].

The introduction of an auxiliary metal is a simple and effective method to improve the performance of Au catalysts. It is well established that the catalytic properties of bimetallic catalysts are usually superior to those of their monometallic counterparts by

taking the advantage of synergistic effect[24][25][26][27]. Thereinto, Au-Cu bimetallic catalysts have received extensive interest in the 'catalysis gold rush'. Owing to the synergistic effect between the two congeners, Au-Cu catalysts usually show enhanced catalytic activity and stability when compared to their monometallic samples[28][29][30][31][32][33]. Not surprisingly, Au-Cu bimetallic catalyst functioned well in acetylene hydrochlorination reaction. For example, Wang et al.[8][34] developed an active Au-Cu/C catalyst. However, active species in this Au-Cu/C tended to sinter during the reaction. Therefore, despite of its high efficiency, industrial application of Au-Cu/C was mainly hindered by its poor stability. Zhang et al.[20] introduced $Co(NH_3)_6Cl_3$ to Au-Cu/SAC catalysts and found that Co could inhibit the carbon deposition obviously and the reduction of Au^{n+} (n = 1 or 3) to Au^0 during the preparation and reaction process. Zhou et al.[9] introduced KSCN into Au-Cu catalyst, and obtained Au-Cu-SCN/AC that had higher activity and stability. Despite of all these achievements abovementioned, the problem of sintering of active species remained unsolved and thus the active structure of Au NPs damaged during the reaction, leading to continuous deactivation. To obtain more stable Au-Cu/AC catalysts, new and effective methods should be proposed to solve the problem of sintering.

As is well known, the catalytic performance of Au featuring catalysts directly depends on their size and structure. The addition of Cu to Au catalysts will definitely enhance the dispersion of gold and produce smaller Au NPs[9][20]. However, owing to their high surface energy, smaller Au NPs are usually unstable, hence they tend to agglomerate during the preparation or reaction process, resulting in a poor activity or

stability. To solve this problem, various physical and chemical approaches have been adopted to stabilize Au NPs. Thiol is one common additive and it has been researched extensively in many cases[35][36][37] including catalysis[23][38]. It was demonstrated that bonding effect between Au and sulfydryl could separate and protect Au NPs. For example, Zhang et al.[35] realized the successful dispersion and stabilization of large Au NPs (20-50 nm) in solution through the use of thiol-based ligands (e.g. 1,1,1-tris(mercaptomethyl)-pentadecane). Gaur et al.[37][38] used C_{12}-SH as additive to synthesize thiol-ligated Au_{38} clusters supported on TiO_2 to catalyze CO oxidation reaction, and improved performance was obtained. On account of these achievements, it's reasonable to imagine that thiol might be effective in preparing stable Au-Cu catalysts for acetylene hydrochlorination reaction. However, thiol can reduce Au^{3+} to Au^0 species to prepare Au^0-based catalyst, which failed to draw broad attentions for acetylene hydrochlorination reaction so far.

In this work, thiol was introduced to develop Au-Cu-SH/AC catalysts that exhibit enhanced catalytic activity and stability than ordinary Au-Cu/AC catalysts. For comparison, the properties of Au-Cu-SH/AC catalysts were characterized and compared with Au/AC and Au-Cu/AC in detail.

2 Experimental

2.1 Materials and reagents

$HAuCl_4 \cdot 4H_2O$ (assay 47.8%), NaOH, hydrochloric acid (36-38%), thioglycollic acid ($C_2H_4O_2S$) were purchased from Guoyao Chemical Reagent Company (Shanghai,

China); $CuCl_2 \cdot 2H_2O$ was purchased from Shanghai Zhanyun Chemical Co., Ltd.; activated carbon (marked as AC, 14–18 mesh) was obtained from Hainan coconut shell activated carbon factory; Nitrogen (99.99%) was purchased from Jingong materials Co., Ltd.; Hydrogen chloride (99.998%) was provided by Shanghai Weichuang Standard Gas Analytical Technology Co., Ltd.; Acetylene (99.5%) was purchased from Jiaxing Tianli Gas Co., Ltd.

2.2 Catalyst preparation

The activated carbon (AC) was initially washed with dilute aqueous HCl (1 mol L^{-1}) at 70 ℃ for 5 h to remove residual alkali species, which may affect the catalyst preparation and final catalytic performance. The mixture was filtered, washed with distilled water till pH=7 and then dried at 140 ℃ for 12 h[7].

The activated carbon-supported Au-Cu catalyst (Au-Cu/AC) was prepared according with the incipient wetness impregnation technique. A certain amount of $HAuCl_4 \cdot 4H_2O$ and $CuCl_2 \cdot 2H_2O$ was dissolved in deionized water to prepare the Au-Cu impregnation liquid. Similarly, a certain ratio of $HAuCl_4 \cdot 4H_2O$ to $CuCl_2 \cdot 2H_2O$ was dissolved in sodium thioglycolate aqueous solution to prepare the Au-Cu-SH impregnation liquid. Thereinto, sodium thioglycolate aqueous solution was prepared by dissolving NaOH into thioglycollic acid aqueous solution, and the molar ratio of NaOH to thioglycollic acid was 2:1. The obtained impregnation liquid was added dropwise to AC under constant shaking. After that, the wet product was kept at room temperature for 2h to gain a better impregnation, and then dried at 140 ℃ for 12h before being collected for use.

The Au content of all catalysts was fixed at 0.5 wt%, and various Cu/Au molar ratios of 0/1, 0.5/1, 1/1, 5/1, 10/1 and 20/1, denoted as Au1Cux/AC (x=0, 0.5, 1, 5, 10, 20), and SH/Cu/Au molar ratios of 0/1/1, 3.5/1/1, 5/1/1, 10/1/1 and 20/1/1, denoted as Au1Cu1SHy/AC (y=0, 3.5, 5, 10, 20) were prepared.

2.3 Catalyst testing

Hydrochlorination reaction of acetylene was carried out in fixed bed laboratory microreactor. Catalysts were tested using a stainless steel reactor tube (i.d. of 8 mm). The reaction zone consisted of 0.5 g fresh sample of catalyst. The reactor was operated at atmospheric pressure, and maintained at 180 ℃, in down-flow mode. N_2 was used as purging gas. Pressure of the reactants, namely HCl and C_2H_2, was chosen for safety and in accordance with industrial condition.

After being heated to 180 ℃, highly purified hydrogen chloride was regulated by mass flow controllers and fed into the reactor alone for 1 h to activate the catalyst, according to the industrial process. Then, acetylene was introduced into concentrated sulfuric acid to remove trace poisonous impurities such as acetone, moisture, S, P and As, and subsequently fed into the reactor to start the reaction.

A total GHSV (gas hourly space velocity) of 2550 h^{-1}, which gave a total MHSV (mass hourly space velocity) of 7.9 h^{-1}, was chosen for catalyst testing. Conversion of acetylene was not too high in this situation (< 75%), thus all results obtained were in kinetic regime[10]. A reactor loaded with 0.5 g bare activated carbon presented only slight activity for hydrochlorination of acetylene (< 0.5% conversion of acetylene). The gas product was passed through a vessel filled with 15% sodium hydroxide solution

and a drying tube in sequence to remove the remaining hydrogen chloride and moisture. The composition of the effluent was determined immediately using a gas chromatography equipped with a flame ionization detector. Catalytic performance was evaluated by conversion of acetylene (X_A), selectivity of VCM (S_{VCM}) and the deactivation rate (DR) as follows:

$$X_A=\varphi_{VCM}\times 100\% \quad \text{(Eqn.1)}$$

$$S_{VCM}=\varphi_{VCM}/(1-\varphi_A)\times 100\% \quad \text{(Eqn.2)}$$

$$DR=-(X_A^L-X_A^H)/t\times 100\% \quad \text{(Eqn.3)}$$

Where φ_A and φ_{VCM} are the volume fraction of remaining acetylene and VCM in gas product separately, X_A^H and X_A^L refer to the highest and the last X_A obtained respectively during the experiment. Time span from X_A^H and X_A^L is denoted as t, in units of hours.

The specific rate of a catalyst was calculated by the following formula[19]:

$$\text{specific rate}=\frac{\text{mol of acetylene converted}}{\text{mass of gold used }(g)\times\text{time }(h)} \quad \text{(Eqn.4)}$$

The induction period was defined as the time last from the start of reaction to the moment that the activity reached the highest and began to decline.

2.4 Catalyst characterization

Morphology of activated carbon carrier was obtained by scanning electron microscopy (SEM) using a Hitachi TM-1000 scanning electron microscope. The samples were deposited on carbon holders and evacuated at high vacuum before micrographs were taken.

The texture properties of the catalysts were derived from N_2 adsorption–desorption measurements carried out at liquid nitrogen temperature using an ASAP2020 instrument. Prior to any adsorption measurements, each sample was outgassed at 200 ℃ for 6 h to eliminate air and vapor from the capillaries of the pore structures of the solids. Specific surface areas and pore volume of the samples were calculated applying BET and T-plot models respectively.

X-ray powder diffraction spectra (XRD) were acquired with a Philips PW3050/60 vertical goniometer using Ni-filtered Cu Kα1 radiation (λ = 1.5406Å). A proportional counter and a 0.02° step size in the 2θ range from 5 to 80°. The assignment of the various crystalline phases is based on the JPDS powder diffraction file cards.

The size of the Au NPs was determined by transmission electron microscopy (TEM). JEM 2100F field emission transmission electron microscope (JEOL) working at 200 kV was used to acquire the images.

Temperature-programmed reduction (TPR) experiments were performed using a Micromeritics AutoChem 2920 instrument equipped with a thermal conductivity detector (TCD). The weight of the tested samples was 0.1 g. The temperature was increased from 50 to 500 ℃ at a heating rate of 10 K min^{-1} with a 10.0% H_2-Ar atmosphere flowing at a rate of 30 mL min^{-1} for TPR. The final temperature of 500 ℃ was maintained for 0.5 h.

The X-ray photoelectron spectroscopy (XPS) analyses were performed by an ESCALAB 250 Xi XPS system (Thermo Fisher Scientific), England and excited by monochromatic Al Kα radiation (1486.6 eV). All binding energies were calibrated

using the C(1s) peak (284.6 eV).

3 Results and discussion

3.1 Effects of Cu content on catalytic performance

The performance of Au-Cu catalysts and the influence of Cu content were firstly studied. In this section, Cu was introduced into Au/AC catalyst to improve the catalytic activity and Au-Cu series catalysts were tested. The content of Au in the catalysts was fixed at 0.5 wt%, while the molar ratio of Cu to Au was varied from 0 to 20.

The catalytic performance of catalysts is shown in Fig. 1 and conversion of acetylene for each catalyst is plotted against time on stream (TOS). The ordinary Au/AC attained conversion of acetylene at about 36.0%, along with a deactivation rate of 0.677% h^{-1}. The highest activity of Au-Cu/AC catalysts increased when the molar ratio of Cu to Au increased gradually from 0 to 5. Whilst, further addition of Cu brought about negative effects, with poorer activity and stability.

According to Pauling's electronegativity principles, Au is more electronegative than Cu[43]. Thus, it is reasonable to assume that electron transfers from Cu to Au and accumulates at the Au center in this Au-Cu bimetallic system, which would be confirmed below. As a consequence, the adsorption of hydrogen chloride at Au was enhanced, which could promote the initial reaction rate and thus shorten the induction period of the reaction. As we can see in Fig. 2, the induction period shortened, as Cu increasing. However, the enhanced adsorption of hydrogen chloride would exacerbate the dispersion of Au NPs and the damage of active structure[19]. Accordingly, it was

discerned that Au-Cu samples in Fig. 1 exhibited poorer stability.

Au1Cu1/AC catalyst showed the best stability and relatively higher activity when the molar ratio of Cu to Au equal 1. Thus, we determined that the optimum molar ratio of Cu to Au is 1, with 50.4% acetylene conversion, 99.9% selectivity to VCM, and the deactivation rate of 0.731% h^{-1}.

3.2 Effects of thiol content on catalytic performance

The performance of Au-Cu-SH catalysts and the influence of thiol content were firstly studied. In this part, thiol was introduced into Au-Cu/AC to prepare Au-Cu-SH/AC catalysts by adding thioglycollic acid. The content of Au was fixed at 0.5 wt%, and the molar ratio of Cu to Au was 1:1, the optimum molar ratio of Cu to Au according to findings listed above, whilst the molar ratio of thioglycollic acid to Au was varied from 0 to 20.

Obtained catalytic performance is shown in Fig. 3. It is immediately evident that as the content of thiol increased, except for Au1Cu1SH20/AC, conversion of acetylene gradually increased. It could be attributed to the thiol which could improve the dispersion of Au. When thiol was excessive, such as in Au1Cu1SH20/AC, the size of active species may be too small to have catalytic activity with reduced active sites[17]. Whilst, it can be observed that the stability of thiol-contained sample became better, with increasing thiol. Such achievements might be ascribed to the stabilization effect of thiol on Au NPs. Experimental results demonstrated Au1Cu1SH10/AC was the most active sample with conversion of acetylene of 56.3%. In the meantime, it was quite stable, with a deactivation rate of 0.178 % h^{-1}.

For convenient comparison, the catalytic performance of Au/AC, Au1Cu1/AC and Au1Cu1SH10/AC is summarized in Table 1 (Fig. S1 and Fig. S2 in detail). It can be observed that the Au1Cu1SH10/AC catalyst showed the highest catalytic activity with about 1.56 times the catalytic activity of ordinary Au/AC catalyst. Specific rate of Au1Cu1SH10/AC reached 13.3 mol g^{-1} h^{-1}. More importantly, the deactivation rate of Au1Cu1SH10/AC was rather smaller, reflecting the extended lifetime. The enhanced activity and stability of Au1Cu1SH10/AC demonstrated that the thiol could be used to improve the catalytic performance of Au-Cu/AC catalysts.

3.3 Property change of Catalysts

To elucidate the in-depth mechanisms that enabled the improvement abovementioned, typical catalysts, namely bared AC, Au/AC, Au1Cu1/AC and Au1Cu1SH10/AC as well as their used samples, were detailedly characterized.

3.3.1 Texture properties

The morphology of pure activated carbon is shown in Fig. S3. As could be discerned, the surface of activated carbon is porous, with no visible impurity. Pore structure parameters of catalysts are shown in Table 2. In comparison with bared activated carbon, the surface area, pore volume and average pore diameter of the three fresh samples decreased respectively in the order of Au/AC, Au1Cu1/AC and Au1Cu1SH10/AC. The change of texture properties might be attributed to the loading active species with additives on the surface of activated carbon. Nevertheless, such tiny surface changes, resulting from the loading of active component, should not be the main causation of the

obvious change of the final performance.

3.3.2 The presence of thiol on the surface of Au NPs

XPS S2p spectrums of fresh Au1Cu/AC and Au1Cu1SH10/AC were shown in Fig. 4. Unsurprisingly, as no sulfur in fresh Au1Cu/AC, there was no any peaks, indicating no sulfur in fresh Au1Cu/AC. Using a 2:1 peak area ratio and a 1.1eV splitting, peak fitting of XPS S2p spectrum of Au1Cu1SH10/AC indicated doublet peaks at 162.2 eV (S $2p_{3/2}$) and 163.3 eV (S $2p_{1/2}$), resulted from sulfur which was bound to Au nanoparticles [38][39][40][41][42]. The peak centered at 167.0 eV can be assigned to oxidized sulfur species [40], produced by the redox reaction between thiol and Au^{3+}. The results indicated that the thiol could reduce Au^{3+} and bond to the surface of Au NPs successfully.

3.3.3 Valence of active species in the fresh samples

H_2-TPR profiles presented in Fig. 5 showed that fresh Au/AC catalyst exhibited a characteristic reduction band in the range of 240 and 300 ℃ assigned to $Au^{\delta+}$ (δ=1, 3). By contrast, there are two characteristic reduction bands in fresh Au1Cu1/AC. The first weaker band, in the range of 200 to 270 ℃, was attributed to $Au^{\delta+}$. In contrast to fresh Au/AC, an evident decrease in the reduction temperature of $Au^{\delta+}$ in fresh Au1Cu1/AC was observed, which meant easier reduction of $Au^{\delta+}$, possibly caused by electron transfer[20]. The area of this peak is small, testifying that only trace amount of Au loaded in the activated carbon was in its oxidation states. Another peak, in the range of 300 to 440 ℃, attributed to $Cu^{\delta+}$ (δ=1, 2), was much stronger, because $Cu^{\delta+}$ has weaker oxidation ability than $Au^{\delta+}$ and is difficult to be reduced just by activated carbon.

No reduction peak was observed in the TPR profiles of fresh Au1Cu1SH10/AC, implying the absence of $Au^{\delta+}$ and $Cu^{\delta+}$. In other words, all Au and Cu element in fresh Au1Cu1SH10/AC was in the form of Au^0 and Cu^0. The same results were revealed by the deconvolution of the XPS spectra shown in Fig. S4 – S9, and the surface relative amount of each Au species and their binding energies are listed in Table 3. The XPS spectra of Au/AC and Au1Cu1/AC both showed Au($4f_{7/2}$) peaks at 84.1(±0.1) and 86.1(±0.3) eV, which could be assigned to Au^0 and Au^{3+}, respectively. Whilst, only Au^0 could be discerned in Au1Cu1SH10/AC. It also indicated the presence of a third state in fresh Au/AC, Au1Cu1/AC and used Au1Cu1SH10/AC with an Au($4f_{7/2}$) peak at 84.6(±0.2) eV, which could be likely assigned to the Au^+ state[17][44][45]. Compared with fresh Au/AC, the peak of Au($4f_{7/2}$) of fresh Au1Cu1/AC shifted to lower binding energy (from 84.2 eV to 84.0 eV), a sign of strong interaction between Au and Cu that Cu transferred electrons to Au, which could explain the negative change of $Au^{\delta+}$ peak location in Fig. 8.

It can be seen that fresh Au/AC, Au1Cu1/AC and Au1Cu1SH10/AC catalyst contained a large amount of Au^0 species at their surface. As was stated in the literatures[46][47], the emergence of Au^0 was associated with the instability of $HAuCl_4$ and the high reducing ability of activated carbon. Apparently, the XPS result of Au1Cu1SH10/AC suggested that thiol could facilitate the complete reduction of $Au^{\delta+}$ and $Cu^{\delta+}$, which could be ascribed to the stronger reducing ability of sulfydryl of thioglycollic acid than activated carbon[35].

3.3.4 Valence change of active species in used samples

As shown in Fig. 6, Characteristic reduction bands of $Au^{\delta+}$ in all three used samples became stronger, which meant more hydrogen need to be consumed and the content of $Au^{\delta+}$ increased in used catalysts. This finding was in accord with the XPS results summarized in Table 3, demonstrating the increasing of Au^{3+} in used samples, in line with the conclusion of our previous study[19]. It could be observed that Au^{+} species in fresh Au/AC disappeared after the reaction, which might be ascribed to the its instability[21]. Unlike Au, the characteristic reduction bands of $Cu^{\delta+}$ in Au1Cu1/AC and Au1Cu1SH10/AC catalysts changed inconspicuously after the test. Such phenomenon could be attributed to the reason that Au was the main active center and the reactants were mainly adsorbed on the surface of Au NPs.

In comparison with Au/AC and Au1Cu1/AC, the amount of Au^{3+} in Au1Cu1SH10/AC was little and increased less after the test, while it deactivated in a slower rate. This suggested that the emergence of Au^{3+} might be unfavorable while Au^{0} species made more contributions to the catalytic performance in Au1Cu1SH10/AC, in accord with our previous work[19]. Au^{0} species ignored by many researchers could also exhibit more excellent catalytic activity than Au^{3+} species, which was interesting and worth of being explored more deeply in the following studies.

3.3.5 Distribution of active species in the fresh samples

Fig. 6 is the comparison of XPS Au4f spectrums of fresh Au/AC, Au1Cu/AC and Au1Cu1SH10/AC, the signal of thiol-introduced sample was the strongest. Since XPS is a surface technique, the signal is a function of the surface to bulk atoms ratio[48]. Thus we concluded that the best Au dispersion at the surface was obtained in

Au1Cu1SH10/AC, which illustrated that thiol could contribute to the improvement of Au dispersion.

XRD patterns of activated carbon and fresh Au1Cu1SHx/AC (x=0, 3.5, 5, 10, 20) catalysts are shown in Fig. 7. The broad peaks in the range of 2θ = 40~48° typical of carbon materials were observed in the XRD pattern of activated carbon, implying the amorphous framework. The peaks at 2θ of 38°, 44.3°, 64.5° and 77.5° were also observed in the XRD pattern attributed to the 111, 200, 220, and 311 diffractions of face-centered cubic (FCC) metallic gold (JCPDS PDF-04-0784), indicating that reduction of Au^{3+} in the process of catalyst preparation. The presence of Au^{0} in the catalysts cohered with the H_2-TPR and XPS results above-mentioned. However, there was no discernible reflection of Cu or $CuCl_2$ in the XRD patterns, which might because that Cu was well dispersed at the surface of AC[49].

Investigating the Au-Cu-SH/AC series catalysts, we noticed that the Au(111) peak shrunk gradually along with the increasing addition of thioglycollic acid. According to XRD technology, Au NPs with the size below 4 nm and $Au^{\delta+}$ species had invisible XRD signals. One noticed that there were no $Au^{\delta+}$ species in all thiol-introduced samples (H_2-TPR results in Fig. S10), therefore, we can conclude that the amount of Au NPs with the size below 4 nm increased with the increasing addition of thioglycollic acid.

These above results show that the sulfydryl of thioglycollic acid could improve the dispersity of Au^{0} species and prevent the Au NPs from agglomeration during the preparation process of the catalysts, which could be attributed to the function that sulfydryl of thioglycollic acid could bond to the surface of Au NPs and isolate neighbor

particles.

3.3.6 Distribution of active species in used samples

Fig. 8 displays the XRD patterns of fresh and used Au/AC, Au1Cu1/AC and Au1Cu1SH10/AC catalysts. Compared to the fresh samples, the Au(111) peaks of used Au/AC and Au1Cu1/AC shrunk respectively. There was nearly no loss of Au during a short time period in the laboratory testing[9][20]. So it may be the reason that the surface of Au NPs was oxidized by HCl and even the crystalline grains were further broken up into smaller size below 4nm under the effect of feed gas[19][50][51]. Thus, the active structure of Au NPs was damaged and decreased. However, the shrinking phenomenon of Au(111) peak in fresh and used Au1Cu1SH10/AC was not obvious. It was because that thiol could bond to the surface of Au NPs, stabilizing and protecting Au NPs from oxidation of Au NPs surface by HCl. It further avoided consequent structure damage of Au NPs.

TEM pictures of the six samples were presented in Fig. 9. Active species in fresh Au/AC agglomerated obviously. The dispersity was better in fresh Au1Cu1/AC and Au1Cu1SH10/AC. The average particle size of active species in fresh Au1Cu1SH10/AC was 12.8 nm, smaller than 24.9 nm in fresh Au1Cu1/AC shown in Fig. S11. It hardly found any Au NPs under TEM in used Au/AC and Au1Cu1/AC, testifying the speculation that the active species were dispersed into smaller size below 4 nm. However, a great amount of nanoparticles were still observed in used Au1Cu1SH10/AC. The average particle size of nanoparticles in used Au1Cu1SH10/AC was slightly smaller than fresh Au1Cu1SH10/AC, indicating that the dispersion of

crystalline grain still happened during the reaction, but it was inhibited at the extreme. All the TEM results highly coincided with XRD results and supported the conclusion about the function of thiol.

4 Conclusions

Au-Cu-SH/AC catalysts were prepared and exhibited better catalytic performance than Au/AC and Au-Cu/AC catalysts. The optimum molar ratio of Au/Cu/SH was 1:1:10. With a specific rate up to 13.3 mol g^{-1} h^{-1}, Au1Cu1SH10/AC catalyst appeared to be 1.56 times as active as the ordinary Au/AC catalyst and over 99.9% selectivity to VCM. More important, on account of the introduction of thiol, the stability of Au1Cu1/AC catalyst was improved and the rate of deactivation was lowered 76%, which means the lifetime of Au-Cu/AC catalyst could be extended.

It was demonstrated that Au-Cu-SH/AC catalysts were Au0-based catalysts, due to thiol can reduce Au^{3+} to Au^{0} species during the preparation process, and Au^{0} species exhibited more excellent catalytic activity than Au^{3+} species for acetylene hydrochlorination, according to the comparison with the composition of active species in different samples through XPS. Through XRD, TEM and TPR, it was confirmed that the sulfydryl of thiol could bond to the surface of Au NPs, avoiding the agglomeration during the preparation process and mitigating the oxidation of Au^{0} by HCl. It helped protecting Au NPs from structure damage, stabilizing Au NPs in a nearly constant particle size and keeping more active structure under the reaction ambience. Thus, better active species dispersity and active structure protection of Au NPs resulted in better catalytic activity and stability of Au-Cu-SH/AC.

What's more important is that Au^0 species with a specific surface structure and grain size ignored by many researchers in previous studies could also exhibit more excellent catalytic activity than Au^{3+} species. The work proposes a new thought and direction to develop Au-based catalysts for acetylene hydrochlorination.

Acknowledgments

The authors gratefully acknowledge the support and encouragement of National Natural Science Foundation of China (21176208), National Basic Research Program of China (2012CB720500) and Fundamental Research Funds for the Central Universities (2011QNA4032).

Appendix A. Supplementary material

Supplementary data associated with this article can be found, in the online version, at xxxx.

References

[1] The China Plastics Industry Editorial Office, China Bluestar Chengrand Chemical Co. Ltd., Progress of the World's Plastics Industry in 2013-2014, China Plastics Industry, 2015,43(3): 1-40.

[2] China Chloro-Alkali Industry Association. The 12th Five-Year Plan of Chloro-Alkali Industry in China. China Chem. Ind. News 2011, 7 (in Chinese).

[3] Ren, W., L. Duan, Z. Zhu, W. Du, Z. An, L. Xu, C. Zhang, Y. Zhuo, C. Chen. Environmental Science & Technology, 2014, 48(4): 2321-2327.

[4] Trotus, I.T., T. Zimmermann, F. Schuth. Chemical Reviews, 2014, 114(3): 1761-1782.

[5] Shinoda, K. Chemistry Letters 1975, 4(3): 219-220.

[6] Hutchings, G.J. Journal of Catalysis, 1985, 96(1): 292-295.

[7] Tian, X., G. Hong, Y. Liu, B. Jiang, Y. Yang. RSC Advances, 2014, 4(68): 36316-36324.

[8] Wang, S., B. Shen, Q. Song. Catalysis Letters, 2010, 134(1): 102-109.

[9] Zhou, K., J. Jia, C. Li, H. Xu, J. Zhou, G. Luo, F. Wei. Green Chemistry, 2014.

[10] Nkosi, B., N.J. Coville, G.J. Applied Catalysis, 1988, 43(1): 33-39.

[11] Hutchings, G.J.M. Haruta. Applied Catalysis a-General, 2005, 291(1-2): 1-1.

[12] Hutchings, G.J.M. Haruta. Applied Catalysis a-General, 2005, 291(1-2): 2-5.

[13] Hashmi, A.S.K.G.J. Hutchings. Angewandte Chemie-International Edition, 2006, 45(47): 7896-7936.

[14] Carabineiro, S.A.C., L. Martins, M. Avalos-Borja, J.G. Buijnsters, A.J.L. Pombeiro, J.L. Figueiredo. Applied Catalysis a-General, 2013, 467: 279-290.

[15] Rodrigues, E.G., S.A.C. Carabineiro, J.J. Delgado, X. Chen, M.F.R. Pereira, J.J.M. Orfao. Journal of Catalysis, 2012, 285(1): 83-91.

[16] Onal, Y., S. Schimpf, P. Claus. Journal of Catalysis, 2004, 223(1): 122-133.

[17] Conte, M., C.J. Davies, D.J. Morgan, T.E. Davies, A.F. Carley, P. Johnston, G.J. Hutchings. Catalysis Science & Technology, 2013, 3(1): 128-134.

[18] Wittanadecha, W., N. Laosiripojana, A. Ketcong, N. Ningnuek, P. Praserthdam, J.R. Monnier, S. Assabumrungrat. Applied Catalysis A: General, 2014, 475: 292-296.

[19] Tian, X., G. Hong, B. Jiang, F. Lu, Z. Liao, J. Wang, Y. Yang. RSC Advances, 2015, 5, 46366 - 46371.

[20] Zhang, H., B. Dai, W. Li, X. Wang, J. Zhang, M. Zhu, J. Gu. Journal of Catalysis, 2014, 316(0): 141-148.

[21] Zhou, K., W. Wang, Z. Zhao, G. Luo, J.T. Miller, M.S. Wong, F. Wei. Acs Catalysis, 2014, 4(9): 3112-3116.

[22] Conte, M., A.F. Carley, G. Attard, A.A. Herzing, C.J. Kiely, G.J. Hutchings. Journal of Catalysis, 2008, 257(1): 190-198.

[23] Pu, Y., J. Zhang, X. Wang, H. Zhang, L. Yu, Y. Dong, W. Li. Catalysis Science and Technology, 2014, 4(12): 4426-4432.

[24] H. L. Jiang and Q. Xu, J. Mater. Chem., 2011, 21, 13705–13725.

[25] D. Wang and Y. Li, Adv. Mater., 2011, 23, 1044–1060.

[26] M. Sankar, N. Dimitratos, P. J. Miedziak, P. P. Wells, C. J. Kiely and G. J. Hutchings, Chem. Soc. Rev., 2012, 41,8099–8139.

[27] Liu, X.-W. Langmuir, 2011, 27(15): 9100-9104.

[28] Zhang, L., H.Y. Kim and G. Henkelman. The Journal of Physical Chemistry Letters, 2013. 4(17): 2943-2947.

[29] Yuan, X., J. Zheng, Q. Zhang, S. Li, Y. Yang, J. Gong. AIChE Journal, 2014, 60(9): 3300-3311.

[30] B. L. Zhu, Q. Guo, X. L. Huang, S. R. Wang, S. M. Zhang, S. H. Wu and W. P. Huang, J. Mol. Catal. A: Chem., 2006, 249, 211–217.

[31] A. Sandoval, C. Louis and R. Zanella, Appl. Catal., B, 2013, 140–141, 363–377.

[32] C. D. Pina, E. Falletta and M. Rossi, J. Catal., 2008, 260, 384–386.

[33] T. Pasini, M. Piccinini, M. Blosi, R. Bonelli, S. Albonetti, G. J. Hutchings and F. Cavani, Green Chem., 2011, 13, 2091–2099.

[34] Wang, L., B.X. Shen, R.F. Ren, J.G. Zhao. in 2013 3rd International Conference on Mechanical Materials and Manufacturing Engineering, ICMMME 2013, October 1, 2013 - October 2, 2013. 2014. Shanghai, China: Trans Tech Publications Ltd.

[35] Zhang, S., G. Leem, L.-O. Srisombat, T.R. Lee. Journal of the American Chemical Society, 2008, 130(1): 113-120.

[36] Kang, J.S.T.A. Taton. Langmuir, 2012, 28(49): 16751-16760.

[37] Gaur, S., H.Y. Wu, G.G. Stanley, K. More, C. Kumar, J.J. Spivey. Catalysis Today, 2013, 208: 72-81.

[38] Gaur, S., J.T. Miller, D. Stellwagen, A. Sanampudi, C.S.S.R. Kumar, J.J. Spivey. Physical Chemistry Chemical Physics, 2012, 14(5): 1627-1634.

[39] M. C. Bourg, A. Badia and R. B. Lennox, The Journal of Physical Chemistry B, 2000, 104(28): 6562-6567.

[40] Y. Joseph, I. Besnard, M. Rosenberger, B. Guse, H. G. Nothofer, J. M. Wessels, U. Wild, A. Knop-Gericke, D. S. Su, R. Schlogl, A. Yasuda and T. Vossmeyer, J.

Phys. Chem. B, 2003, 107(30): 7406-7413.

[41] Maye M. M., Luo J, Lin Y, Engelhard M. H. Langmuir, 2003, 19(1):125-131.

[42] Castner D. G., Hinds K., Grainger D. W. Langmuir, 1996, 12(21):5083-5086.

[43] Yuan, X., J. Zheng, Q. Zhang, S. Li, Y. Yang, J. Gong. AIChE Journal, 2014, 60(9): 3300-3311.

[44] Sham, T.K., A. Hiraya, M. Watanabe. Physical Review B, 1997, 55(12): 7585-7592.

[45] Buono, C., P.R. Davies, R.J. Davies, T. Jones, J. Kulhavy, R. Lewis, D.J. Morgan, N. Robinson, D.J. Willock. Faraday Discussions, 2014, 173(0): 257-272.

[46] Chen, S.X.H.M. Zeng. Carbon, 2003, 41(6): 1265-1271.

[47] Bulushev, D.A., I. Yuranov, E.I. Suvorova, P.A. Buffat, L. Kiwi-Minsker. Journal of Catalysis, 2004, 224(1): 8-17.

[48] Conte, M., C.J. Davies, D.J. Morgan, T.E. Davies, D.J. Elias, A.F. Carley, P. Johnston, G.J. Hutchings. Journal of Catalysis, 2013, 297: 128-136.

[49] Han, M.S., B.G. Lee, B.S. Ahn, D.J. Moon, S.I. Hong. Applied Surface Science, 2003, 211(1-4): 76-81.

[50] Nkosi, B., M.D. Adams, N.J. Coville, G.J. Hutchings. Journal of Catalysis, 1991, 128(2): 378-386.

[51] Zhang, J., Z. He, W. Li, Y. Han. Rsc Advances, 2012, 2(11): 4814-4821.

Table 1 Comparison of fresh Au/AC, Au1Cu1SH/AC and Au1Cu1SH10/AC.

Catalysts	initial activity/%	Selectivity/%	Deactivation rate/%h^{-1}
Au/AC	36.0	99.92	0.677
Au1Cu1/AC	50.4	99.88	0.731
Au1Cu1SH10/AC	56.3	99.92	0.178

Reaction conditions: Temp=180 ℃;GHSV(C_2H_2)=1200 h^{-1};V_{HCl}/V_{C2H2}=1.13.

Table 2 Pore structure parameters of samples.

Catalysts	AC	Au/AC	Au1Cu1/AC	Au1Cu1SH10/AC
BET Surface area[(a)]	888.8	841.4	834.2	785.4
Pore volume[(b)]	0.465	0.445	0.428	0.377
Ave. pore diameter[(c)]	2.12	2.14	2.08	1.94

Units in the table: (a) m^2/g, (b) cm^3/g, (c) nm.

Table 3 Surface relative amount and binding energies of Au^{3+}, Au^{+} and Au^{0} over Au/AC, Au1Cu1/AC and Au1Cu1SH10/AC catalysts determined by XPS.

Catalysts	Au^0		Au^+		Au^{3+}	
	Binding energy[(a)]	Oxidation state[(b)]	Binding energy[(a)]	Oxidation state[(b)]	Binding energy[(a)]	Oxidation state[(b)]
Au/AC- fresh	84.2	48.9	84.8	46.1	86.0	5.0
Au/AC- used	84.0	57.1	--	--	86.4	42.9
Au1Cu1/AC- fresh	84.0	71.7	84.4	21.7	85.8	6.6
Au1Cu1/AC- used	84.0	42.4	--	--	86.4	57.6
Au1Cu1SH10/AC-fresh	84.2	100.0	--	--	--	--
Au1Cu1SH10/AC-used	84.1	59.6	84.8	18.6	86.6	21.8

Units in the table: (a) eV, (b) %.

Figure captions

Fig. 1 Effects of Cu content on the catalytic performance of Au-Cu/AC series catalysts. Reaction conditions: Temp=180 ℃; GHSV(C_2H_2)=1200 h^{-1}; V_{HCl}/VC_{2H2}=1.13.

Fig. 2 Induction Period of Au-Cu/AC series catalysts.

Fig. 3 Effects of thiol content on the catalytic performance of Au-Cu-SH/AC series catalysts. Reaction conditions: Temp=180 ℃ ; GHSV(C_2H_2)=1200 h^{-1}; V_{HCl}/VC_{2H2}=1.13.

Fig. 4 XPS S2p spectrum of fresh Au1Cu1/AC and Au1Cu1SH10/AC catalysts.

Fig. 5 H_2-TPR profiles of Au/AC, Au1Cu1/AC and Au1Cu1SH10/AC fresh and used catalysts.

Fig. 6 XPS Au4f spectrums of fresh Au/AC, Au1Cu1/AC and Au1Cu1SH10/AC catalysts.

Fig. 7 XRD patterns of Au1Cu1SHy/AC series fresh catalysts.

Fig. 8 XRD patterns of Au/AC, Au1Cu1/AC and Au1Cu1SH10/AC fresh and used catalysts.

Fig. 9 TEM picture: (a)Au/AC-fresh; (b)Au/AC-used; (c)Au1Cu1/AC-fresh; (d)Au1Cu1/AC-used; (e)Au1Cu1SH10/AC-fresh; (f)Au1Cu1SH10/AC-used.

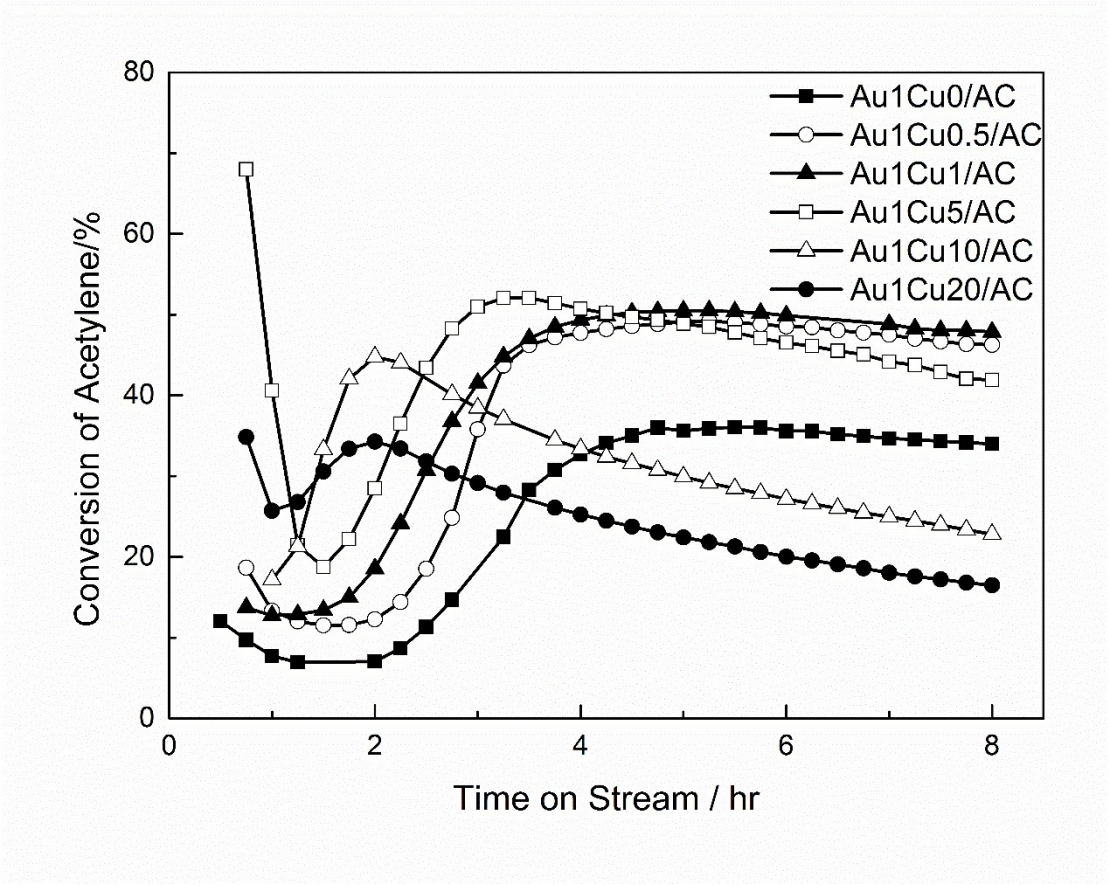

Fig. 1

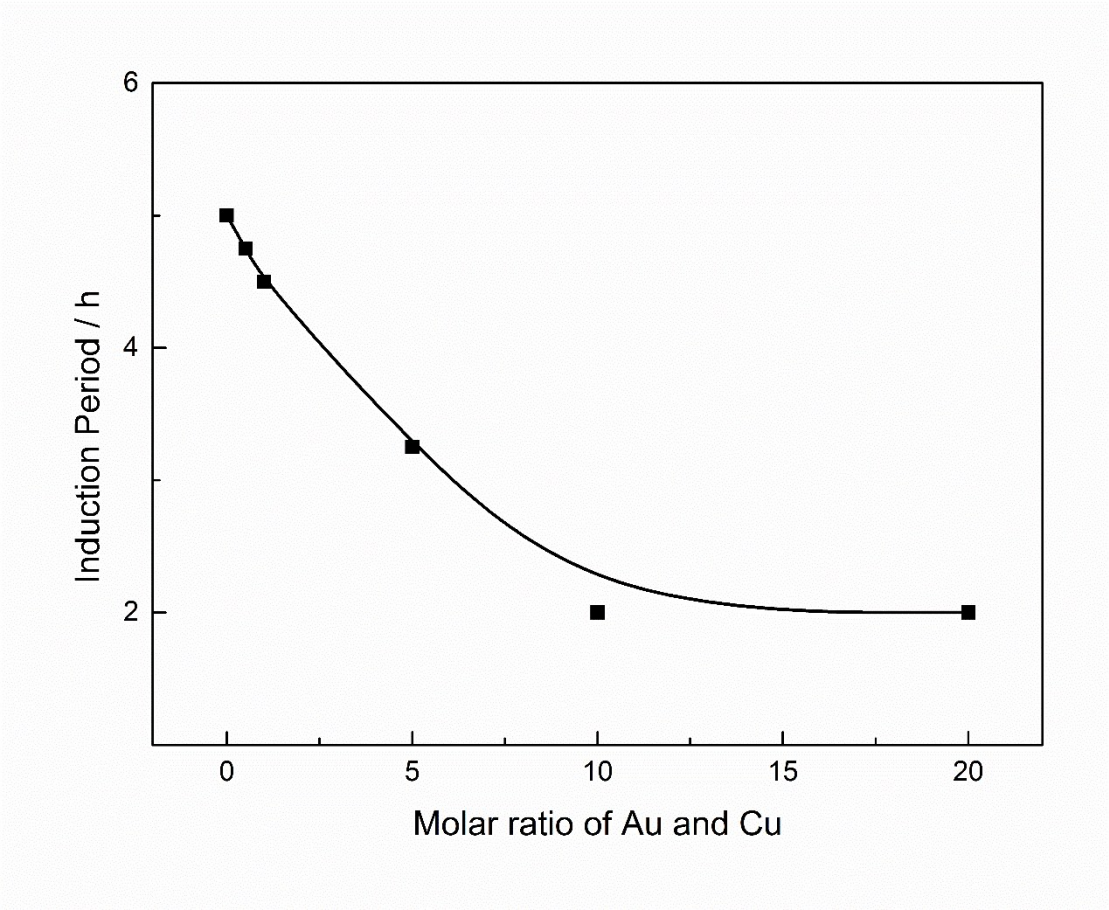

Fig. 2

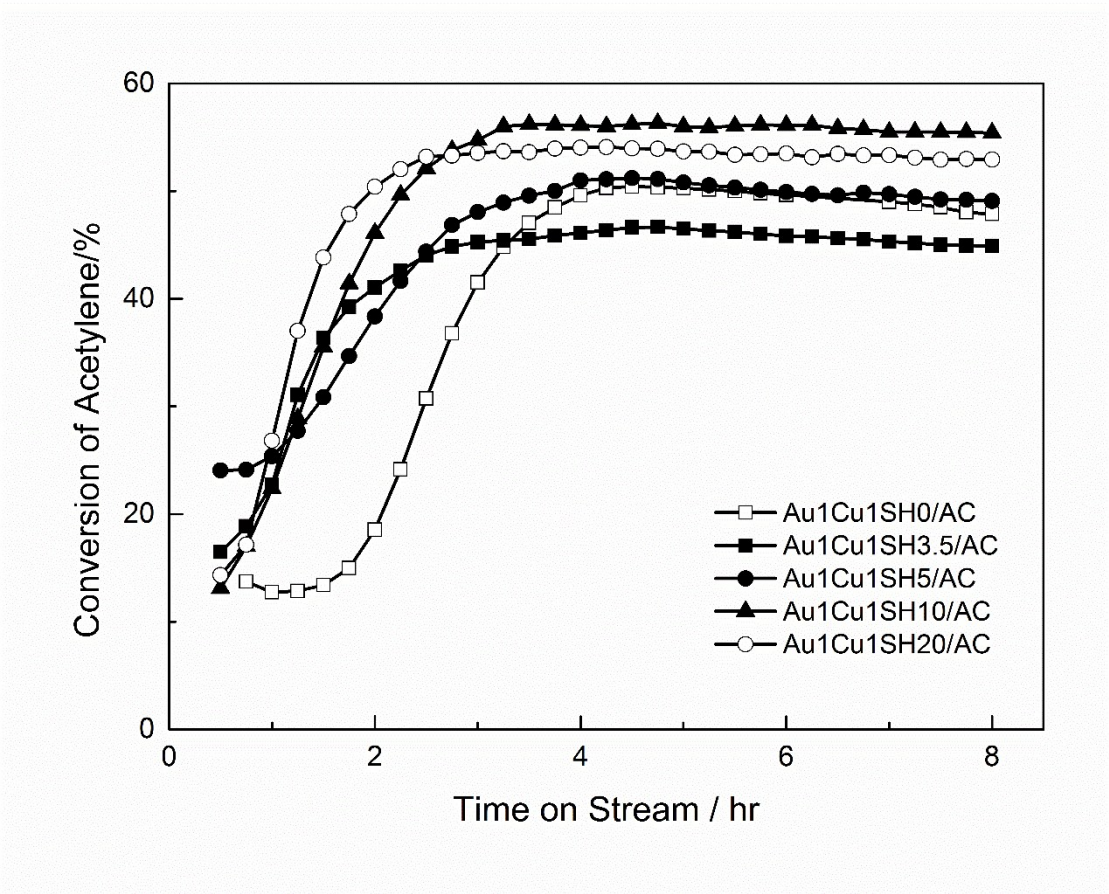

Fig. 3

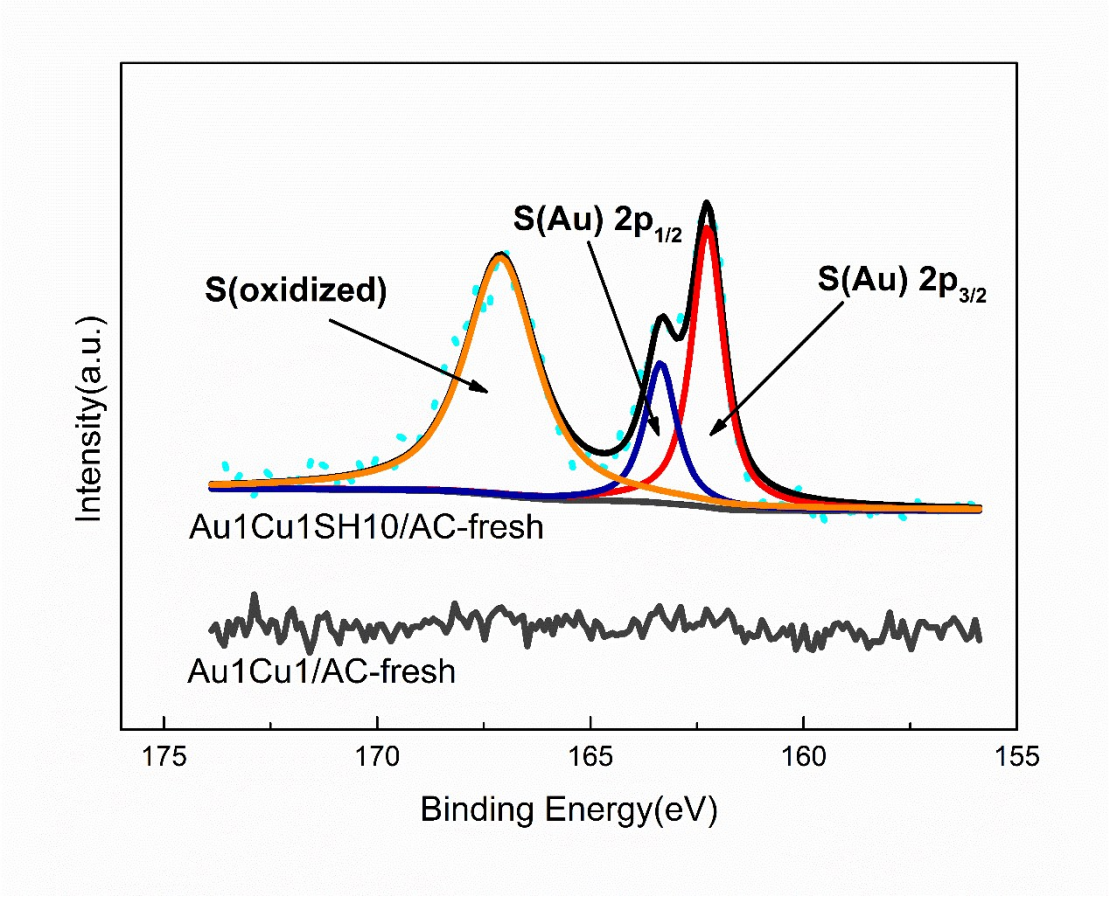

Fig. 4

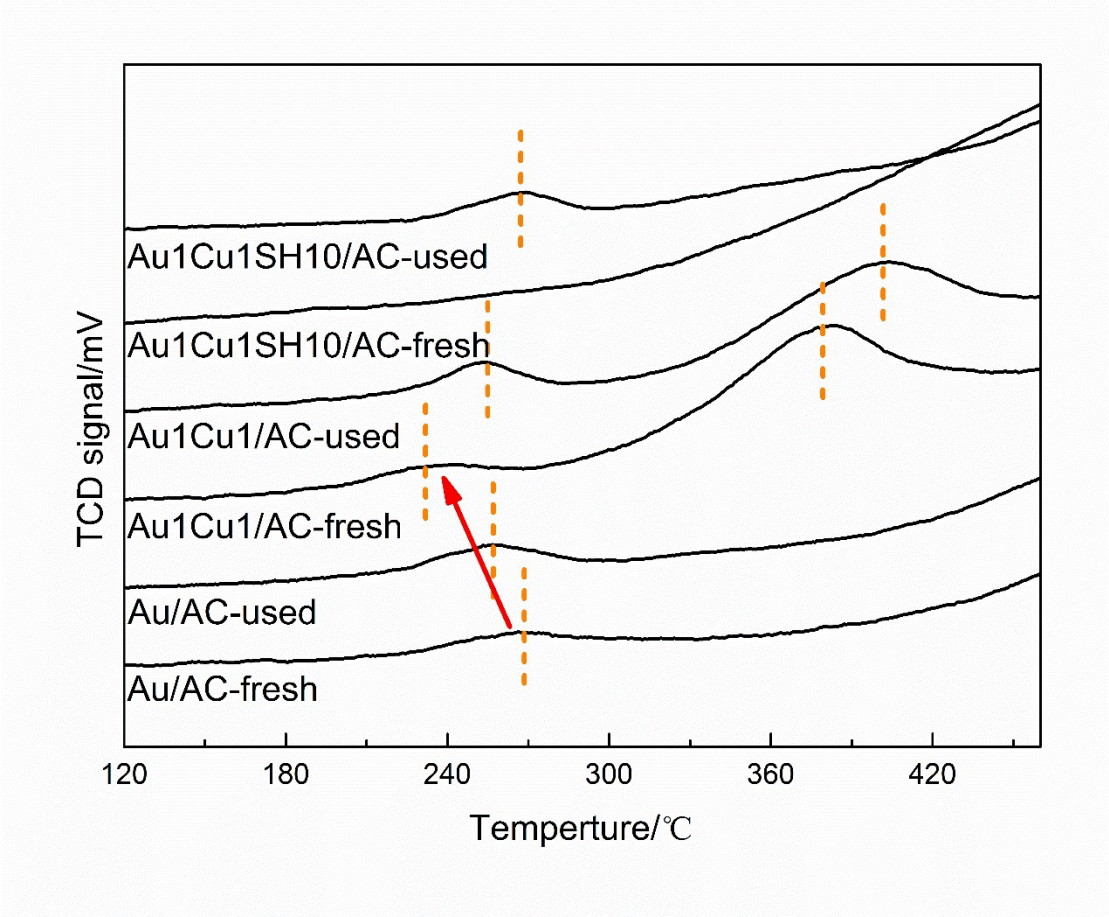

Fig. 5

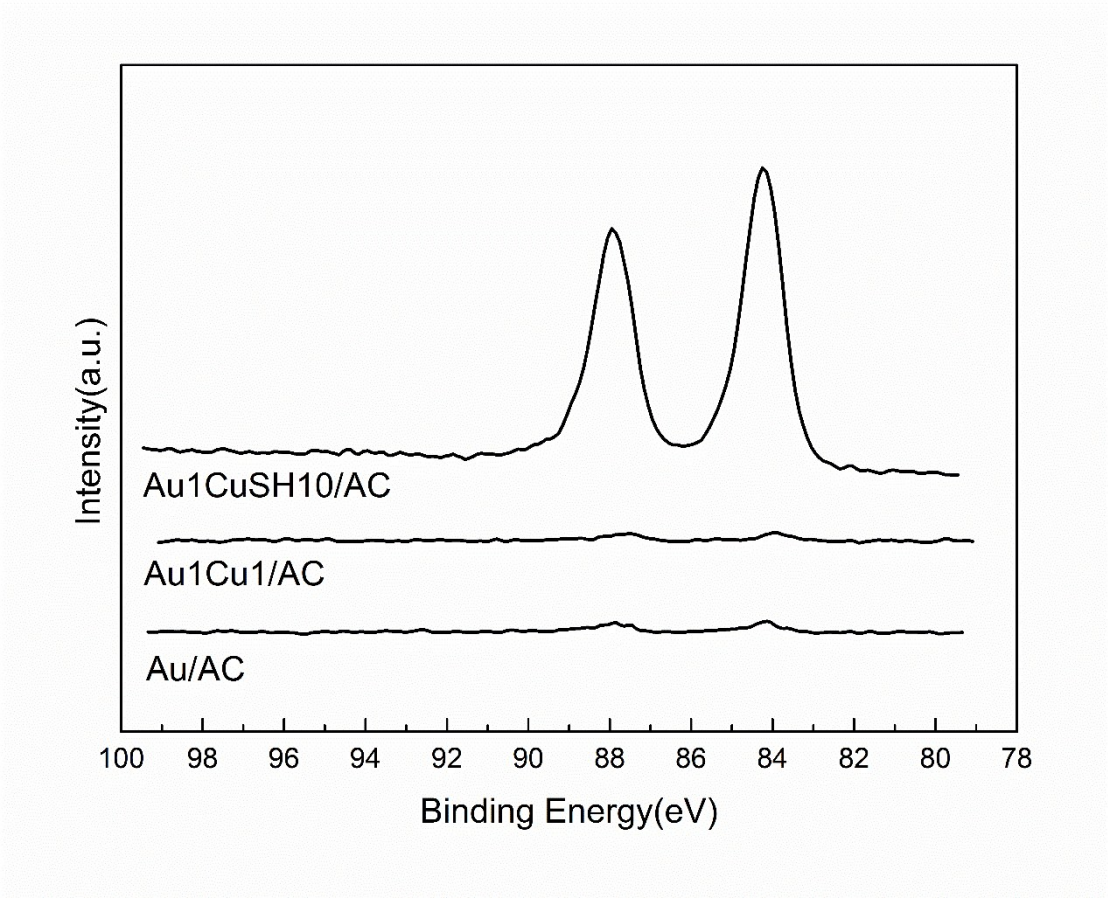

Fig. 6

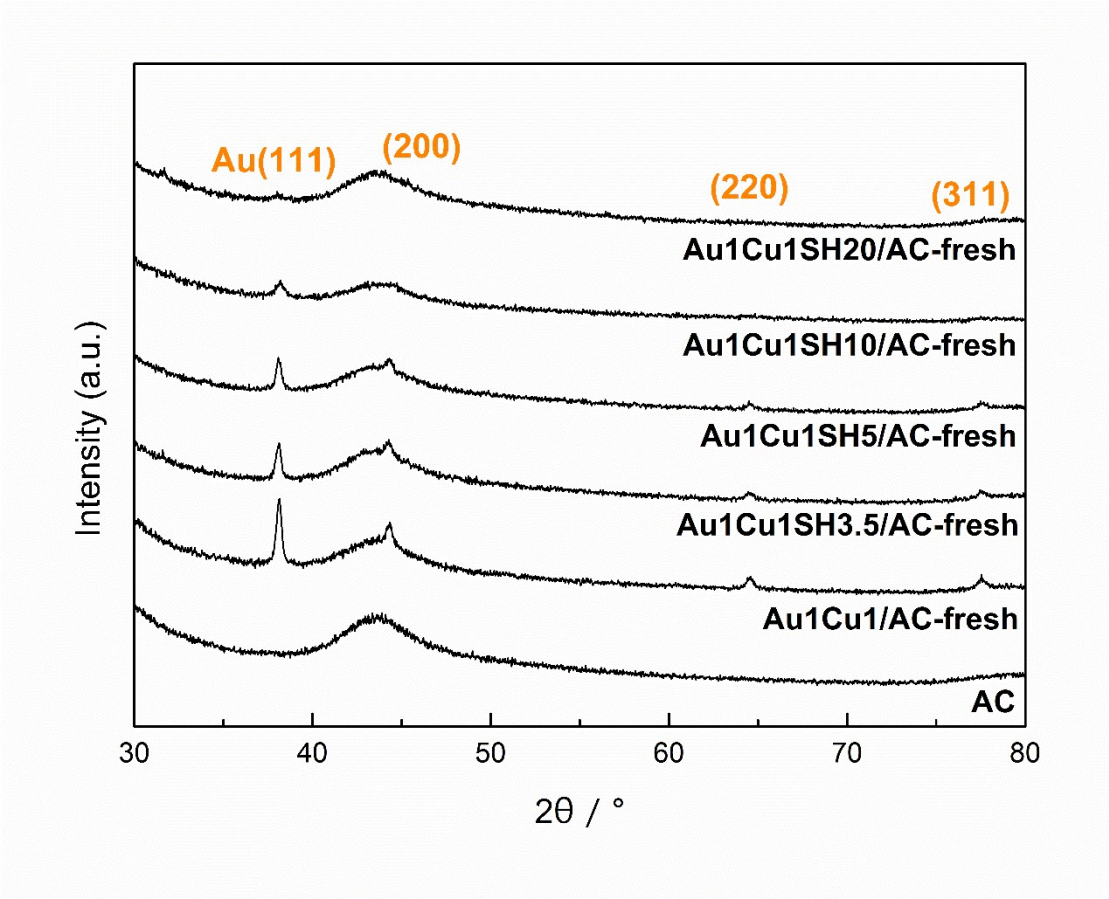

Fig. 7

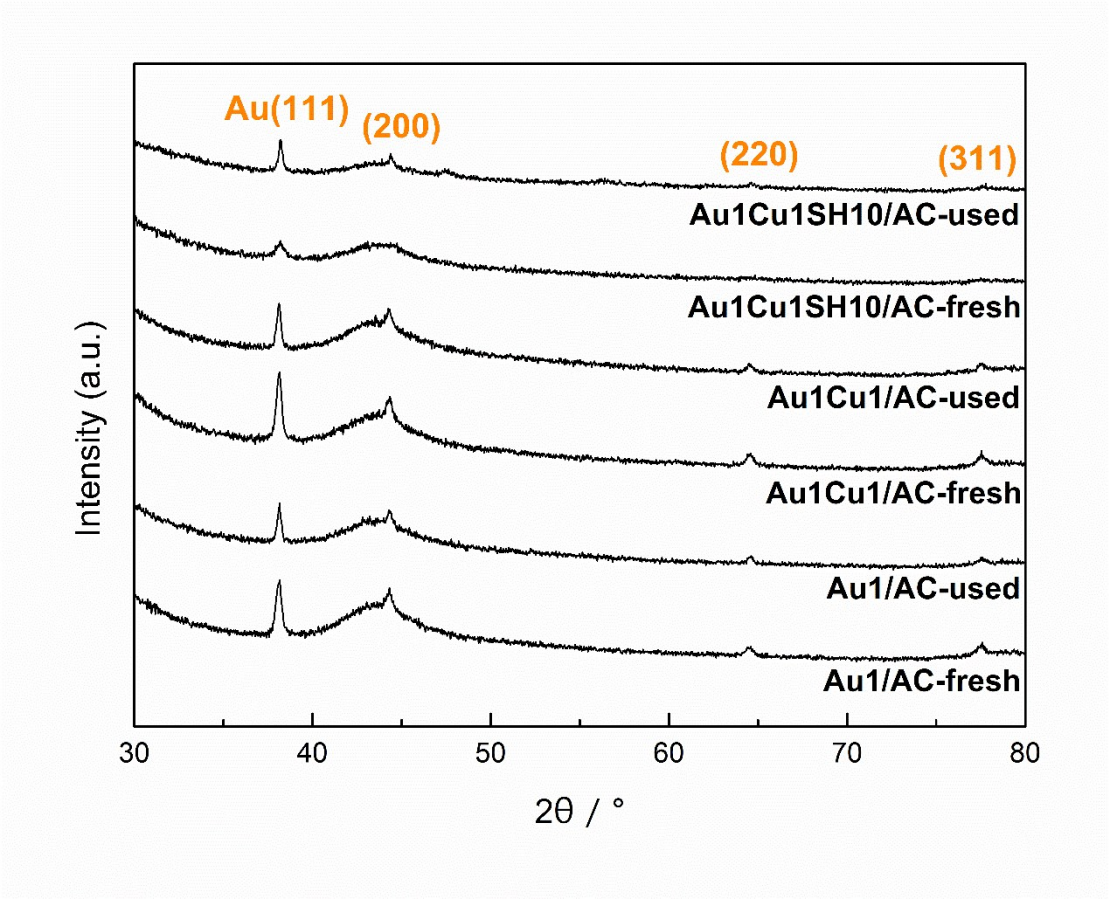

Fig. 8

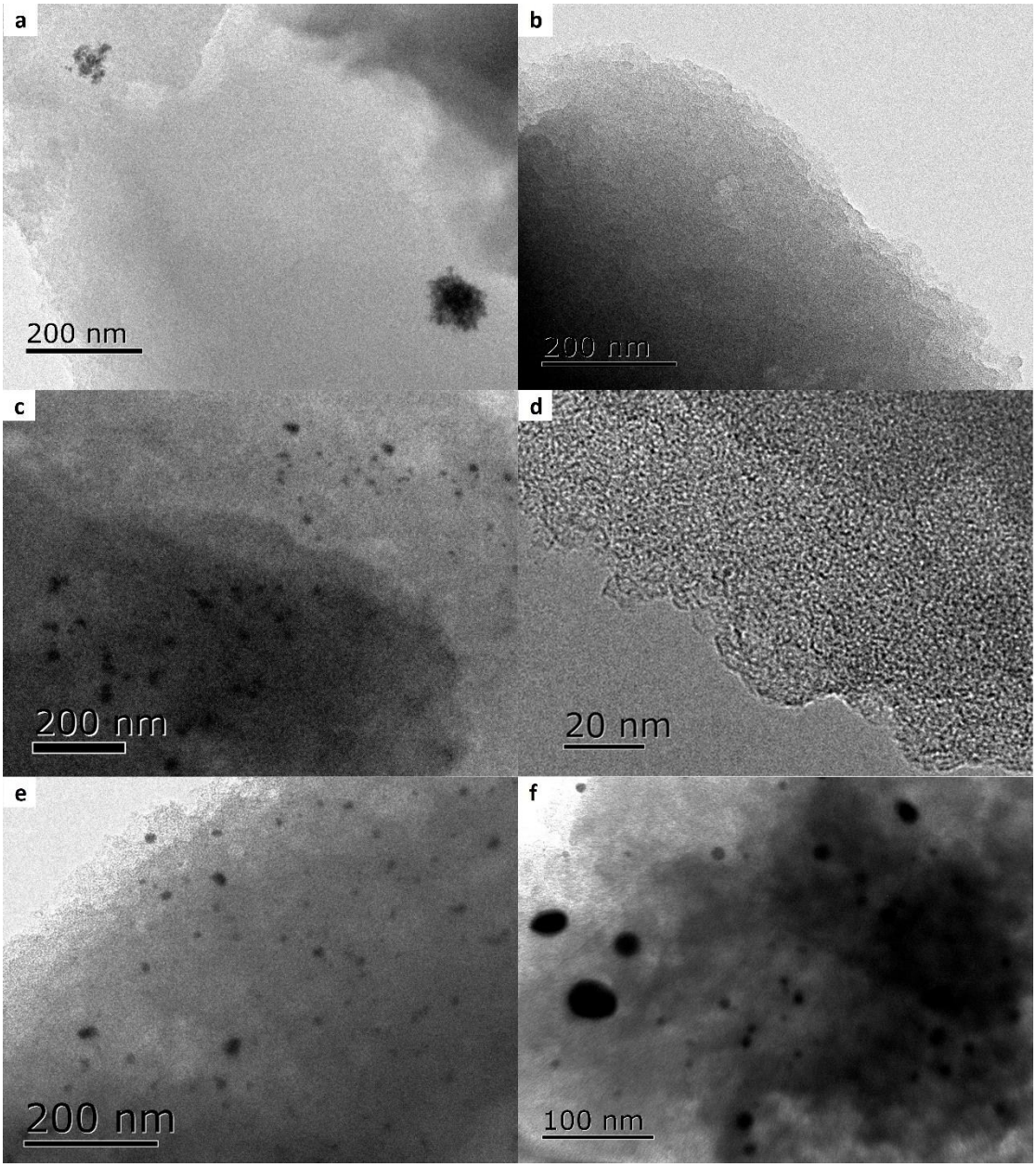

Fig. 9

Improvement of performance of Au-Cu/AC catalyst using thiol for acetylene hydrochlorination reaction

Guotai Hong[a], Xiaohui Tian[a], BinBo Jiang[*a], Zuwei Liao[a], Jingdai Wang[a], Yongrong Yang[ab], Jie Zheng[c]

[a.]State Key Laboratory of Chemical Engineering, College of Chemical and Biological Engineering, Zhejiang University, Hangzhou 310027, Zhejiang, China

[b.]Shanghai Key Laboratory of Catalysis Technology for Polyolefins, Shanghai 200062, China

[c.]Department of Chemical and Biomolecular Engineering, The University of Akron, Akron, Ohio, USA 44325

Graphical Abstract

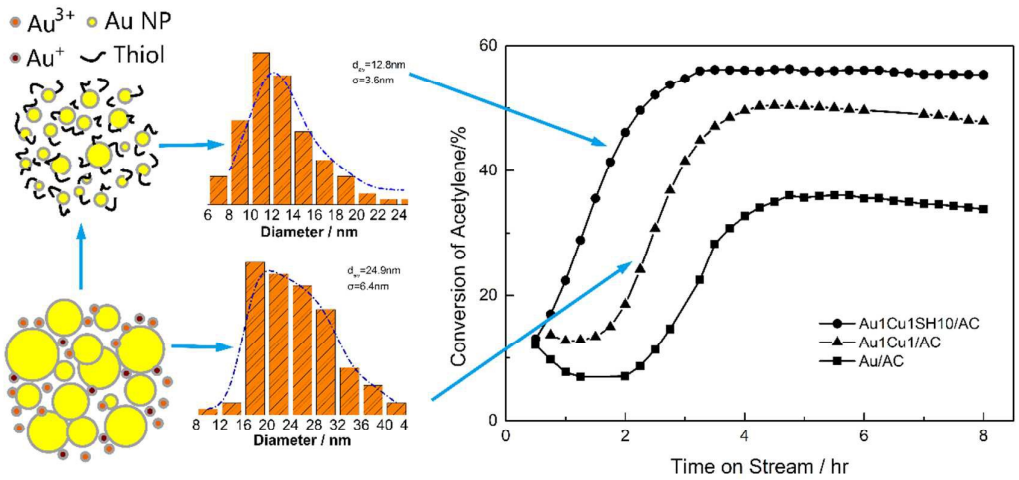

Thiol could bond to the surface, mitigating the oxidation by HCl and protecting the active structure of Au NPs.